1458

Gaussian mixture based Hidden Markov Models for analysis of task fMRI dynamics

Pavithran Pattiam Giriprakash MS[1], Dr. Chendi Han PhD[1], Dr. Xiaowei Zhuang PhD[1], Dr. Zhengshi Yang PhD[1], Dr. Rajesh Nandy PhD[2], Dr. Katherine A Koenig PhD[3], Dr. Mark J Lowe PhD[3], Dr. Dietmar Cordes PhD[1,4]

[1]Cleveland Clinic Lou Ruvo Center for Brain Health, Las Vegas, NV, United States. [2]University of North Texas Health Science Center, Fort Worth, TX, United States. [3]Imaging Institute, Learner Research Institute, Cleveland Clinic, Cleveland, OH, United States. [4]Department of Psychology and Neuroscience, University of Colorado, Boulder, CO, United States

INTRODUCTION

Brain activity is inherently dynamic, constantly evolving to support information processing during task and rest. Hidden Markov models (HMMs) characterize this dynamic behavior as a sequence of probabilistic transitions between a finite set of latent states, where each state has its own connectivity pattern[1]. Unlike sliding window methods that depend on an arbitrary window size, HMMs can be used to capture faster state transitions that happen during tasks. As a result, they have seen widespread application in task fMRI, particularly in paradigms focusing on dynamic high-level cognitive processes such as working memory, episodic memory and attention-based tasks. The default mode network (DMN) and fronto-parietal networks (FPN) have been widely recognized to have a competitive, anti-correlation relationship during tasks[2]. The DMN (internal focus) and FPN (external attention) interact dynamically with the DMN typically suppressed and FPN being activated, a relationship modulated by several factors including task demands, age, disease state. A pattern separation task measures the brain activity when participants distinguish between similar but distinct stimuli, measuring the ability to decode overlapping inputs as distinct memories. Thus, it is particularly essential for episodic memory retrieval. Previous works have considered the hippocampus and the CA3/dentate gyrus to be the regions most important for pattern separation. Recently, the FPN was also found to exhibit distinct activation patterns during pattern separation[3]. Left lateralized activations were involved in object pattern separation while right FPN contributed to retrieval of previously encoded stimuli. However, the dynamic relationship of FPN with other networks, specifically, the DMN has largely been unexplored. In this abstract, we propose to utilize a Gaussian mixture HMM to analyze the temporal dynamics of the interaction between FPN and DMN during the recognition period of a pattern separation task.

METHODS

A total of 87 participants were enrolled in the study, distributed across 2 groups, specifically, 46 with normal cognition (NC) and 41 patients with mild cognitive impairment (MCI). MRI data were acquired on a 7T Siemens Magnetom Terra scanner using a 32-channel head coil. Each fMRI session was collected using a multi-band gradient echo EPI sequence with 1.5mm isotropic voxel size, 81 slices, TR = 1530ms, TE = 22ms, flip angle = 70 degrees, echo spacing = 0.67 ms and 510 timepoints. A total of 3 task fMRI sessions were collected from each participant. In addition, T1 MP2-RAGE and GRE field mapping scans were also collected.

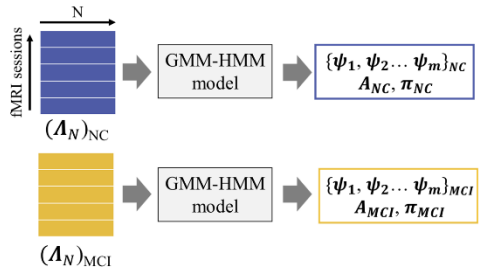
The object pattern separation task used in the study consisted of three phases, namely, encoding, recognition and distraction. During encoding, 66 visual stimuli were presented and the subject responded whether the stimuli was an indoor or outdoor object. During recognition phase, 86 objects were presented which were (a) same as the ones presented during encoding (22/86), (b) similar to encoding stimuli but distinct (44/86) or (c) completely new (20/86). The subjects responded if the objects seen were same (target), similar (lures) or new (foil). Complete details of the task are discussed in[3].

fMRI data were preprocessed as follows: slice-timing correction, realignment and distortion correction. A Gaussian smoothing filter with 4mm FWHM was applied. The smoothed data were coregistered to the T1 space and spatially normalized to the MNI 2mm space. The preprocessed data had dimensions 510 x 91 x 109 x 91. The timeseries from the voxels within the brain were extracted resulting in a 510 x 228453 feature dimension. A group Independent Component Analysis (ICA) based on FastICA[4] with tanh nonlinearity was performed on the temporally concatenated data from all the subjects to obtain 15 independent components. Then, 2 representative networks, one each for DMN and FPN were shortlisted for subsequent analysis. Subject-level data were then back-reconstructed using GIG-ICA[5]. The timeseries from these 2 networks belonging only to the recognition phase (T = 292 timepoints) were used as inputs for the Gaussian mixture based HMM (GMM-HMM) model.

Each hidden state was represented by a Gaussian mixture with parameters (w_i, μ_i, Σ_i) as seen in Figure 1. The initial parameter estimates were randomly initialized and a standard Expectation-Maximization (E-M) algorithm was used to maximize the log-likelihood. Since parameters estimated E-M algorithms are influenced by initial values, 20 random realizations were run and the run yielding the maximum log-likelihood was used for subsequent analysis. A multisequence model was run separately for both the groups to estimate both the HMM parameters (A, π) and GMM parameters (w_i, μ_i, Σ_i). HMM being unsupervised, the states obtained from different processes are not guaranteed to match across realizations. Thus, a so-called Hungarian algorithm was run for 100 permutations for matching the states across the groups, NC and MCI. Briefly, it found the assignment that maximized

the correlation between the posterior state activation probabilities from the two groups. The number of hidden states that resulted in the lowest values of the information criteria scores, AIC and BIC were chosen as the optimal value. Viterbi algorithm was used to decode for the most likely hidden state at each timepoint. Then, the dFC parameters, fractional occupancy, mean sojourn time and switching rate were estimated for each session and compared across groups. Effect sizes based on Cohen's d (d) were utilized to compare the means across NC and MCI.

METHODS FIGURE (OPTIONAL)



GMM-HMM model

Objective	$\max \mathcal{L}^e(\boldsymbol{\Theta}\|\boldsymbol{\Lambda_N})$	
$\mathcal{L}^e(\boldsymbol{\Theta}\|\boldsymbol{\Lambda_N}) = \sum_{j=1}^{N} \log\left(p(\boldsymbol{\lambda}_j\|\boldsymbol{\Theta})\right)$; where, $p(\boldsymbol{\lambda}_j\|\boldsymbol{\Theta}) = \sum_{i=1}^{M} w_i \mathcal{G}(\boldsymbol{\lambda}_j, \boldsymbol{\mu}_i, \sum_i)$		
HMM parameters		
State transition matrix	$\boldsymbol{A} \in \mathcal{R}^{m\,X\,m}$	$\sum_i A_{ij} = 1$ and $A_{ij} \geq 0$
Initial state probability	$\boldsymbol{\pi} \in \mathcal{R}^{m\,X\,1}$	$\sum_i \pi_i = 1$ and $\pi_i \geq 0$
GMM parameters $\boldsymbol{\Theta} = \{\boldsymbol{\psi}_1, \ldots, \boldsymbol{\psi}_M\}$ *and* $\boldsymbol{\psi}_i = \{w_i, \boldsymbol{\mu}_i, \sum_i\}$		
Mixture weights	$w_i \in \mathcal{R}^{M\,X\,1}$	$\sum_i w_i = 1$ and $w_i \geq 0$
Mixture means	$\boldsymbol{\mu_i} \in \mathcal{R}^{M\,X\,D}$	
Mixture covariance	$\sum_i \in \mathcal{R}^{M\,X\,D\,X\,D}$	$\sum_{reg} = \sum_{orig} + \alpha I$

D – Dimensionality of the Gaussian functions
N – Timepoints
m – Number of hidden states
M – Number of gaussians in a GMM

dFC features

Viterbi path: $Q = \{q_1, q_2, \ldots, q_T\}$
Set of possible states: $S = \{1, 2, \ldots, m\}$
Indicator function: $\mathbb{I}(\cdot)$

Fractional occupancy (FO)	$FO_k = \frac{1}{T}\sum_{t=1}^{T} \mathbb{I}(q_t = k)$
Mean sojourn time (MST)	$V_k = \{d_{k,1}, d_{k,2}, \ldots, d_{k,N_k}\}$ $MST_k = \frac{1}{N_k}\sum_{i=1}^{N_k} d_{k,i}$
Switching rate (SR)	$SR = \frac{1}{T-1}\sum_{t=1}^{T-1} \mathbb{I}(q_t \neq q_{t+1})$

Figure 1: Group-specific Gaussian mixture based Hidden Markov model and parameter estimation with the objective of maximization of log-likelihood. Three dynamic functional connectivity (dFC) features were estimated, namely, fractional occupancy, mean sojourn time and switching rate from the Viterbi path.

RESULTS

Figure 2(a) shows that the E-M algorithm reliably converged across different random seeds, as shown by the negligible variance in the final log-likelihood values in the final iteration. Prior to applying the Hungarian algorithm, the states were not matched across NC and MCI as shown by the negative correlations (-0.70, -0.03, -0.38 and -0.20) between their state activation probabilities as seen in figure 2(b). Whereas, in the after plot, all the correlations showed strong positive correlations (> 0.8 for states 1, 2 and 4). When optimizing for the number of brain states, a total 5 different brain states (2, 3, 4, 5 and 6) were evaluated using the AIC and BIC criterion. Both the metrics identified 6 as the optimal number of hidden states.

In terms of dFC, NC subjects showed a significantly higher mean switching rate (SR) compared to the MCI patients (d = 1.04). This was also accompanied by a lower mean sojourn time (MST) in the NC compared to MCI for all the states. In particular, state 2 showed significantly higher MST in MCI with a large effect size (d = 1.19) whereas state 1 showed a medium effect size (d = 0.67). With respect to fractional occupancy, states 1 and 6 showed a higher fractional occupancy in NC compared to MCI with medium effect sizes (d = 0.57 and d = 0.64 respectively). In contrast, state 2 showed an opposite trend with the MCI showing higher FO (d = 0.55). The estimated groupwise estimates of the Gaussian mixture parameters also showed differences. The following interpretations are made relative to the dominant Gaussian in the mixture. For state 2, the mean activation for both FPN and DMN where close to zero for the dominant Gaussian. For state 1, mean of DMN is close to zero whereas FPN is positive. Mean of DMN is close to zero and FPN is negative for state 6. The states also showed difference in the interaction between the two networks which is captured by the off-diagonal elements in the covariance matrix. The tilted ellipses in states 1, 3, 4 and 6 reflected a positive relationship between DMN and FPN. State 5 indicated a state where the networks are functionally independent from one another. State 2 with the highest FO, near zero mean for DMN and FPN could indicate a stable baseline state. States 1 and 6 with near zero mean for DMN whereas positive and negative mean for FPN potentially reflect distinct task states that subjects transition to complete the necessary task load.

RESULTS FIGURE (OPTIONAL)

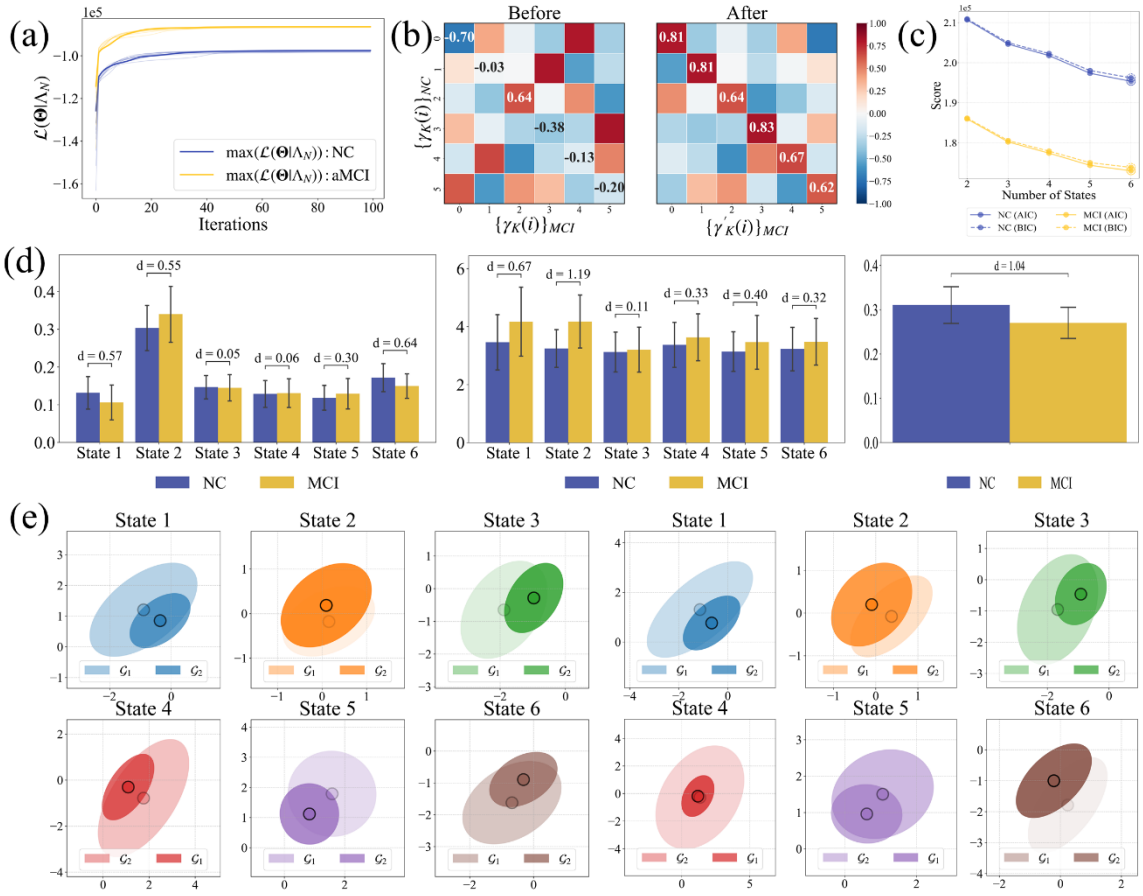


Figure 2: (a) shows the log-likelihood across 100 iterations for multiple random initializations, (b) shows the increased positive correlation between the state probabilities after running Hungarian, (c) depicts the optimal choosing of number of hidden states using BIC and AIC, (d) shows the different dFC parameters extracted, (e) GMM parameters (means, weights and covariances) across NC and MCI.

CONCLUSION

In conclusion, we have utilized Gaussian mixture HMMs to reveal distinct hidden states characterized by unique mean and covariance structures between the default mode and fronto-parietal networks. Also, group specific alterations in dynamic functional connectivity were observed. The task dynamics, represented by the dFC features indicated that a healthy aging brain in NC are able to better adapt to changing cognitive demands during the task by occupying states briefly and switching to different state configurations more rapidly. Whereas, MCI subjects, however, cannot adapt to task dynamics and get stuck in certain states much longer indicative of disease related cognitive processing deficits. The model performance was currently evaluated using the entire dataset and thus needs to be cross-validated in the future. Also, the homogenous HMM used in this study would be expanded into a non -homogenous setup to include time-varying

estimates of transition matrix, impact of covariates on both HMM and GMM parameters in future work.

REFERENCES/CITATIONS

1. Vidaurre D, Abeysuriya R, Becker R, et al. Discovering dynamic brain networks from big data in rest and task. NeuroImage. 2017;180(Pt B):646-656. doi:10.1016/j.neuroimage.2017.06.077
2. Rossi C, Vidaurre D, Costers L, et al. A data-driven network decomposition of the temporal, spatial, and spectral dynamics underpinning visual-verbal working memory processes. Communications Biology. 2023;6(1):1079. doi:10.1038/s42003-023-05448-z
3. Yang Z, Zhuang X, Koenig KA, et al. Pattern separation involves regions beyond the hippocampus in non-demented elderly individuals: A 7T object lure task fMRI study. Imaging Neuroscience. 2024;2:1-15. doi:10.1162/imag_a_00404
4. Hyvarinen A. Fast and robust fixed-point algorithms for independent component analysis. IEEE Transactions on Neural Networks. 1999;10(3):626-634. doi:10.1109/72.761722
5. Du Y, Fan Y. Group information guided ICA for fMRI data analysis. NeuroImage. 2012;69:157-197. doi:10.1016/j.neuroimage.2012.11.008

ACKNOWLEDGEMENT

This work was supported by NIH grants, R01AG071566 and P20GM109025.